

Statistical analysis of offshore wind turbine failures

Wanwan Zhang

Department of mechanical and industrial engineering, NTNU, Norway. E-mail: wanwan.zhang@ntnu.no

Jørn Vatn

Department of mechanical and industrial engineering, NTNU, Norway. E-mail: jorn.vatn@ntnu.no

Adil Rasheed

Department of Engineering Cybernetics, NTNU, Norway. E-mail: adil.rasheed@ntnu.no

This paper aims to investigate the characteristics of offshore wind turbine failures. Four hypotheses on failure features are proposed and strictly examined by statistical tests. Cox model is chosen to model failure process. Three forms of co-variables are designed to research their influence on failures. Their coefficients are obtained by maximum likelihood estimation and Breslow estimator is calculated. Finally, goodness-of-fit tests verify the assumptions of Cox model. Results of long-term models show that wind significantly favors the growth of baseline hazard. However, temperature and production condition mildly reduce it. The effects will gradually become stable if accumulation time increases. Similar results are observed in models with principal components of co-variables. Comparison of models suggest the highest likelihood belongs to models with three accumulated co-variables.

Keywords: Hypotheses testing, Cox model, offshore wind turbine, failure process, accumulated co-variables

1. Introduction

Failures of offshore wind turbines (OWTs) are influenced by many different factors such as environment, maintenance, and turbine technologies (Cevasco et al., 2021). Among all factors, environmental loads is the key to design effective maintenance strategies on offshore system (Adumene and Ikue-John, 2022). This paper aims to explore failure properties of OWTs and quantify the influence of environment on failures.

From 2000 to 2017, connections between environment and wind turbine failures are investigated by traditional statistical techniques. Applied stochastic processes include Homogeneous Poisson Process (HPP) and non-homogeneous Poisson Process (NHPP), especially Power Law Process (PLP). Recently machine learning has been applied to quantify weather influence (Reder et al., 2018).

Nevertheless, most researches are based on onshore databases and not directly applicable to OWTs (Li et al., 2022). The main challenge in offshore area is data availability. Although supervisory control and data acquisition (SCADA) is

applied, high-quality offshore failure data is still scarce in the public domain. To fulfill the research gap, this paper attempts to investigate:

- the stochastic process that best explains the failure associated with a single offshore turbine
- the influence of wind, temperature, power condition on errors of offshore turbines
- the extent to which the accumulation duration of environment influences the baseline hazard

The rest of paper is organized as follows: Section 2 elaborates researches in OWTs failures. Section 3 introduces data and hypotheses. Methods for tests and models are summarized in section 4. Section 5 provides results and discusses them. Conclusions are in section 6.

2. Literature review

Earlier in the 2000s, Tavner et al. study turbine failures based on onshore data from Windstats. HPP and PLP are used to fit data in his work. there is a 44% cross-correlation between the wind index and failure rate with 95% confidence level (Tavner et al., 2006, 2007). Factors that Tavner has

confirmed include rated power, maximum temperature, location, wind turbulence, wind speed and humidity etc. Among them, maximum wind speed has the closest correlation with failures (Tavner et al., 2013).

As Kaidis et al. summarize in 2015, probability distribution is suitable for non-repairable system and point process applies to describe repairable systems. Their research of onshore SCADA data uses Weibull distribution for major repairs and PLP model for manual restarts and minor repairs. It is proposed that bathtub curve should not be taken for granted on turbine failures.

Slimacek and Lindqvist states that it is hard to figure out cause-effects of heterogeneous factors on wind turbines by traditional HPP and there possibly exists unobserved factors. They develop NHPP with nonparametric frailty and covariates and test them on onshore turbines in WMEP database (Slimacek and Lindqvist, 2016a,b, 2017). Results show that coefficients of environment have a seasonal effect on failure process. Besides, they verify the improvement of wind turbine technology over the years.

Except stochastic processes, non-parametric mixture models are also applied to explore the relationship between weather and UK onshore farms (Wilson and McMillan, 2013). They conclude failure probabilities of controller system and drive train models increase with wind. Correlation analysis from Su et al. show that power index and failure rate have similar periodicity and strong correlation. Data mining and apriori rule mining techniques also succeed to find that relative humidity, ambient temperature, wind speed has a relation with failures in critical components (Reder et al., 2018).

Overall, most researches are based on onshore wind turbine data. HPP, PLP and NHPP are suitable candidates for failure data analysis with external factors. However, there lacks researches on OWTs. Secondly, model selection is not clearly presented in researches. Besides, quantification of weather effects are generally calculated on a wind farm level. To deal with the gap, this paper presents a systematic analysis on failures of OWTs with environmental influence.

3. Hypotheses and data

3.1. Hypotheses

Four hypotheses are listed based on literature review. Three variables are selected, maximal wind, average temperature, total power.

- H1.0: Failure process does not have a trend.
- H2.0: The trend is monotonic.
- H3.0: Three variables does not have an effect on failure process.
- H4.0: Accumulation duration does not influence coefficients of variables.

3.2. Dataset

EDP (Energias de Portugal) open database^a provides two-year SCADA records from 5 OWTs in the West African Gulf of Guinea (Menezes et al., 2020). 200 failures of turbine T01 are extracted from command records. Signal data records ambient, grid activities and internal state of OWTs every 10 min from 2016 to 2017.

3.2.1. Ambient data

Pair plot of three variables is in figure 1. Average temperature has the minimal correlation with other two variables.

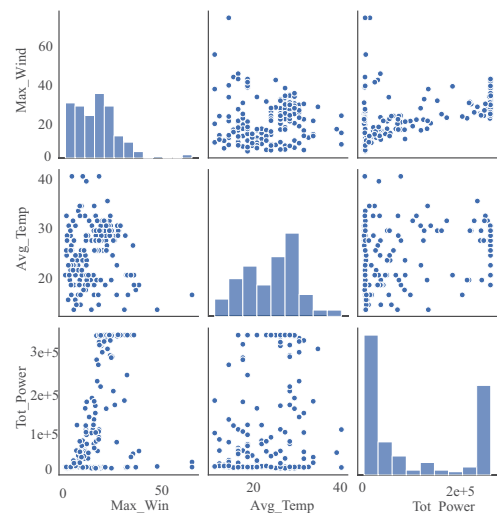


Fig. 1. Pair plots for selected variables

^a<https://www.edp.com/en/innovation/edp-open-data>

3.2.2. Failure data

Failure is defined as the occurrence of error event (Wilkinson and Hassan, 2011). Failures are event logs that are solved by remote, automatic, or manual restarts (Carroll et al., 2016). Stream of failures satisfies a counting process $\{N_t, t \geq 0\}$. Cumulative number of failures N_t counts how many events happen in $(0, t]$. Calendar times of failures are denoted as $T_1, T_2, T_3, \dots, T_{200}$. Inter-arrival time X_i is calculated as $X_i = T_i - T_{i-1}$. Figure 2 shows X_i and T_i .

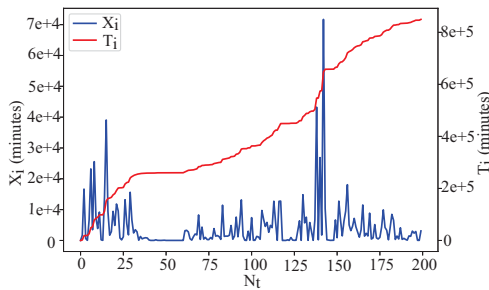


Fig. 2. X_i and T_i over failures

To facilitate plots, $T_0 = 0$ is added to the data stream. Figure 3 plots X_i, N_t , temperature and wind speed over months. The change of temperature and wind over seasons approximately fit tropical climate near the gulf of guinea.

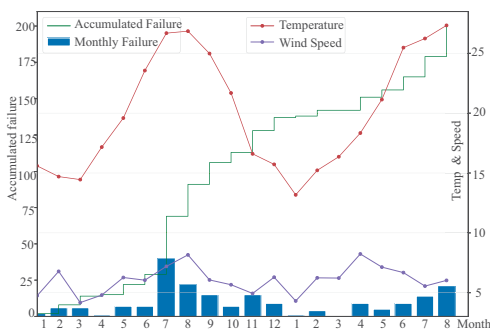


Fig. 3. Monthly view

4. Methods

Figure 4 illustrates the whole procedure of data processing. Four assumptions are examined by trend test, monotonicity tests, parameter estimation. Results from statistical tests provide guid-

ance for model selection and construction.

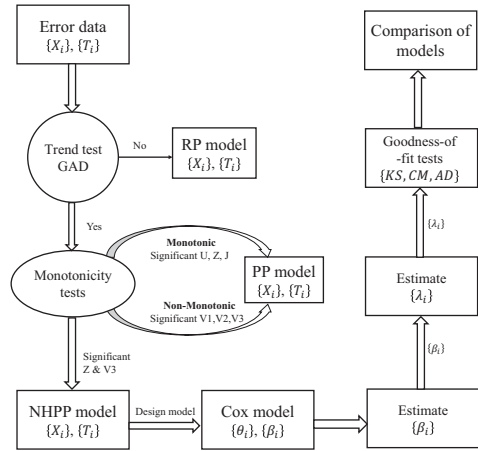


Fig. 4. Flow chart for procedure

4.1. Counting processes and trend test

Trend Renewal Process (TRP), a generalized Renewal Process (RP) with a trend, is introduced to differentiate counting processes. As Kvaløy and Lindqvist point out, all the HPP, RP and NHPP are special cases of TRP. Conditional intensity γ given history \mathcal{F} of TRP is expressed as (Kvaløy and Lindqvist, 2003; Lindqvist et al., 2003):

$$\gamma(t|\mathcal{F}) = z(\Lambda(t) - \Lambda(T_{N(t)}))\lambda(t) \quad (1)$$

In this equation, $\Lambda(t) = \int_0^t \lambda(u)du$. $z(t)$ is a hazard rate function that depends on the system age and the time from the last failure. $\lambda(t)$ is a non-negative trend function. If $\lambda(t)$ is constant, it becomes a RP. Moreover, HPP is the special condition of RP where both $\Lambda(t)$ and $z(t)$ are constant. When $z(t) = 1$, TRP becomes NHPP. Different processes are shown by figure 5.

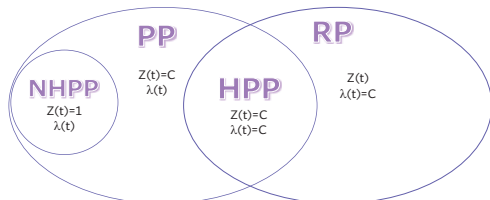


Fig. 5. Properties of processes (Vaurio, 1999)

For trend analysis, generalized Anderson-

Darling (GAD) test based on RP is adopted. GAD has good performance against monotonic and non-monotonic trends (Kvaløy and Lindqvist, 2003).

$$GAD = \frac{n\bar{X}^2}{\hat{\sigma}^2} \sum_{i=1}^n \left[q_i^2 \ln \left(\frac{i}{i-1} \right) + (q_i + r_i)^2 \ln \left(\frac{n-i+1}{n-i} \right) - \frac{r_i^2}{n} \right] \quad (2)$$

Calculation of parameters $q_i, r_i, \hat{\sigma}^2$ is:

$$q_i = \frac{T_i - iX_i}{T_n} \quad (3)$$

$$r_i = \frac{nX_i}{T_n} - 1 \quad (4)$$

$$\hat{\sigma}^2 = \frac{1}{2(n-1)} \sum_{i=1}^n -1(X_{i+1} - X_i)^2 \quad (5)$$

GAD applies a smaller but consistent estimator $\hat{\sigma}^2$ of variance instead of the usual estimator in typical Anderson-Darling (AD) statistic. Thus GAD is more powerful than AD. However, GAD still measures the deviation from a Brownian bridge and has the same limit distribution as AD. Hence, this paper adopts critical values of Brownian bridge from asymptotic tests by Kiefer (Antoch and Daniela, 2007; Kiefer, 1959). They are 0.461, 0.580, 0.743, separately at 5%, 2.5% and 1% significance level.

4.2. Monotonic and non-monotonic tests

For mononicity, Vaurio presents a summary of six statistics for monotonic trends and non-monotonic trends. U, Z, J test monotonic trends. V_1, V_2, V_3 tests non-monotonic trends such as the bathtub curve. The null assumption is that $T_1, T_2, T_3, \dots, T_i$ are uniformly distributed on $(0, T_n]$, which indicates no trend. Under the same assumption, the six statistics follow different distributions. U is laplace test, and Z is Mil-Hdbk-189 test.

$$U = \frac{\sum_{i=1}^n T_i - nT_n/2}{T_n \sqrt{n/12}} \sim N(0, 1) \quad (6)$$

$$Z = 2 \sum_{i=1}^n \log(T_n/T_i) \sim \chi^2(2n) \quad (7)$$

As Vaurio summarizes, U and Z are not always effective especially when the σ is much larger or smaller than mean \bar{X} . Therefore, J is introduced

by changing the numerator of U . J is approximately Student's t-distribution and tests RP versus monotonic trend.

$$J = \frac{\sum_{i=1}^n T_i - nT_n/2}{\sigma[n(n+1)(n+2)/12]^{1/2}} \sim t(n) \quad (8)$$

Still under the same null assumption, V_1 and V_2 obeys standard normal distribution and V_3 is χ^2 distribution. These three statistics have the power to detect non-monotonous failure intensity.

$$V_1 = \frac{\sum_{i=1}^n |T_i - T_n/2| - nT_n/4}{T_n \sqrt{n/48}} \sim N(0, 1) \quad (9)$$

$$V_2 = \frac{\sum_{i=1}^n |T_i - T_n/2|^2 - nT_n^2/12}{T_n^2 \sqrt{n/180}} \sim N(0, 1) \quad (10)$$

$$V_3 = 2 \sum_{i=1}^n \log(T_n/|2T_i - T_n|) \sim \chi^2(2n) \quad (11)$$

4.3. Cox model

4.3.1. Basic assumptions

To construct Cox model, $\{T_i - T_1, 1 \leq i \leq 200\}$ is adopted as input $\{t_i\}$. It represents survival time measured from the calendar time of first error T_1 . In equation 12, maximal wind speed θ_1 , average temperature θ_2 , and total power θ_3 are collected at the nearest time before $\{t_i\}$. $\beta_1, \beta_2, \beta_3$ are parameters to be estimated.

$$\lambda(t) = \lambda_0(t) \exp(\theta\beta) \quad (12)$$

$$\theta = [\theta_1 \ \theta_2 \ \theta_3], \beta = \begin{bmatrix} \beta_1 \\ \beta_2 \\ \beta_3 \end{bmatrix} \quad (13)$$

4.3.2. Parameter estimation

Estimation of coefficients adopts partial log likelihood. This method estimates β without assumptions on $\lambda_0(t)$. The objective function $f(\beta)$ is constructed as follows:

$$f(\beta) = - \sum_{i=1}^n \left[\theta\beta - \ln \sum_i^n \exp(\theta\beta) \right] \quad (14)$$

Minimizing $f(\beta)$ based on β is equal to maximizing partial log likelihood of cox model, which

is a nonlinear optimization problem. Estimated β are used to calculate Breslow estimators $\hat{\lambda}_0(t_i)$ and survival probability $\hat{S}(t_i)$ (Lin, 2007).

$$\hat{\lambda}_0(t_i) = \frac{1}{\sum_i^n \exp(\theta\hat{\beta})} \tag{15}$$

$$\hat{S}(t_i) = \exp\left(-\int_0^{t_i} e^{\theta\hat{\beta}} \hat{\lambda}_0(t) dt\right) \tag{16}$$

4.3.3. Accumulation form of co-variables

s, p, q are the accumulated duration of wind, temperature, and power before failure happens. Because there lacks some weather data, the maximum time for tracing back is 270 minutes. When s, p, q equal to 10 min, 200 failures are fully used to estimate parameters, while the rest can only use 199 failures due to data missing.

$$\theta = \left[\sum_{s=1}^{L_1} \theta_1(s) \sum_{p=1}^{L_2} \theta_2(p) \sum_{q=1}^{L_3} \theta_3(q) \right] \tag{17}$$

4.3.4. PCA form of co-variables

It is likely that co-variables correlation lead to compensation and reduction of parameters. Principle component analysis (PCA) are used to reduce the influence by dividing original information into three uncorrelated principle components (PC). Using all the PCs do not lose any information. New co-variables θ are set to:

$$\theta = [PC0 \ PC1 \ PC2] \tag{18}$$

4.3.5. Goodness of fit tests

Kolmogorov-Smirnov (KS), Cramér-von Mises (CM) and Anderson-Darling (AD) tests are chosen to test proportional assumption of Cox Model. They build on empirical distribution function (EDF) that estimates cumulative distribution function (CDF) step by step (Cockeran et al., 2021). Under the null hypothesis, $\hat{\varepsilon}_1, \hat{\varepsilon}_2, \dots, \hat{\varepsilon}_i$ comes from an exponential distribution. $\hat{\varepsilon}_i$ is calculated:

$$\hat{\varepsilon}_i = \sum_{i=1}^n \frac{\hat{\lambda}_0(i)}{\sum_i^n \exp(\theta\hat{\beta})} \tag{19}$$

Computationally efficient formula are given as follows (D’Agostino and Stephens, 1986):

$$\widehat{KS}_n = \max \{KS_n^+, KS_n^-\} \tag{20}$$

$$KS_n^+ = \max_{1 \leq i \leq n} \left[\frac{i}{n} - (1 - e^{-\hat{\varepsilon}_i}) \right] \tag{21}$$

$$KS_n^- = \max_{1 \leq i \leq n} \left[(1 - e^{-\hat{\varepsilon}_i}) - \frac{i-1}{n} \right] \tag{22}$$

For CM and AD tests, statistics are constructed as follows:

$$CM_n = \frac{1}{12n} + \sum_{i=1}^n \left[(1 - e^{-\hat{\varepsilon}_j}) - \frac{2i-1}{2n} \right]^2 \tag{23}$$

$$AD_n = -n - \sum_{i=1}^n \frac{2i-1}{n} [\ln(1 - e^{-\hat{\varepsilon}_i}) - \hat{\varepsilon}_{n+1-i}] \tag{24}$$

5. Results and discussions

5.1. Statistical tests

Results are given in the table 1. GAD=2.265, which significantly rejects the null assumption **H1.0** that rend is highly significant. Hence, RP is not good for modeling the process. For monotonic tests, only Z and V_3 are significant.

Table 1. Results of 7 statistics

Statistics	Value	p-value
GAD	2.265	<0.01**
U	0.524	0.300
Z	152	2.917e-32***
J	0.286	0.386
V_1	-1.054	0.146
V_2	-0.735	0.231
V_3	182	4.477e-23***

Significance: $p < 0.001\%***, p < 0.01\%**$, $p < 0.1\%*$.

As Vaurio explains, Z and V_3 has the power to determine whether a process is NHPP with power-law type intensity and Weibull type hazard rate. For NHPP with power law intensity, Z and V_3 will follow distribution $\chi(2n)/B$ where B is the power. 5% critical value range for $\chi(2n)$ is [354.6, 447.6]. Because both Z and V_3 falls outside of the lower limit 354.6, B is likely to be larger than 1. Therefore, NHPP model is suitable.

5.2. Cox model

Estimation results for basic model 12 show that β_1 for wind is -0.592, β_2 for temperature is -1.087,

and β_3 for power is 0.306 when accumulation time is 10 min. Three coefficients give the maximal partial log likelihood -858.940. The hypothesis **H3.0** is rejected due to nonzero coefficients.

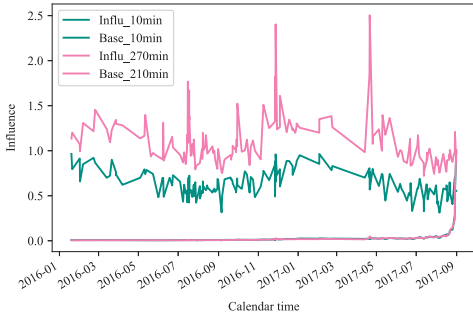


Fig. 6. Baseline hazard and covariates' influence

Figure 6 presents the overall influence $exp(\theta\hat{\beta})$ from covariates on baseline hazard $\lambda_0(t_i)$ over calendar time. Overall influence based on 10-min accumulation is less than 1. However, the influence exceeds 1 if accumulation time is 270 min.

Estimated baseline hazards are similar in both cases. Figure 7 plots the estimated number of errors from two models and the real curve. Three lines are almost overlapped, which suggests Cox model give a good performance of estimation.

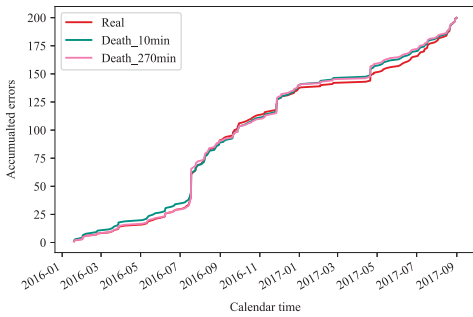


Fig. 7. Comparison of estimation and reality

Table 2 presents the goodness of fit tests for Cox-snell residuals $\hat{\epsilon}_i$. They do not reject the null assumption that $\{\hat{\epsilon}_i\}$ comes from a standard exponential distribution, which satisfies the assumption of Cox model.

Statistics	Origin	PCA	No power
KS	0.036	0.036	0.033
p-value	0.952	0.952	0.980
AD	0.306	0.306	0.282
critical value	0.919	0.919	0.919
CM	0.058	0.058	0.050
p-value	0.830	0.830	0.875

5.3. Comparison of Coefficients

Figure 8 presents coefficients over accumulation time. Temperature keeps a negative influence on hazard growth. If accumulation time is less than 50 minutes, maximal wind speed decreases hazard growth and power production increases it. After 50 minutes, their influences change towards the opposite direction.

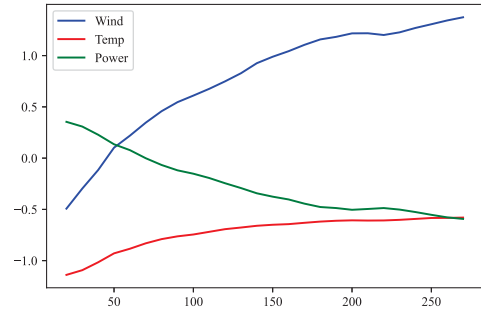


Fig. 8. Coefficients for wind, temp and power

To test the effect of power, test 2 removes power from covariates. Test 1 refers to the model in figure 8. Figure 9 shows the change of coefficients of temperature and wind.

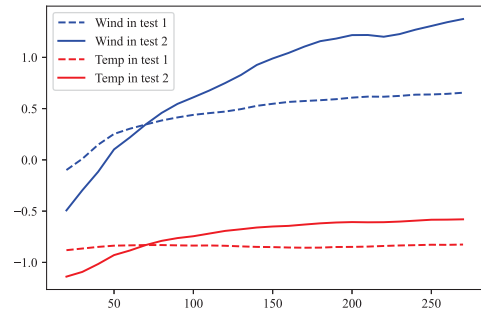


Fig. 9. Coefficients after removing power

Coefficients for PCs are plotted in figure 10. PC0 represents 50% to 60% of total information. PC1 occupies 30% and PC2 has 20% to 10%. PC1 finally obtains changeless negative coefficient. Coefficient of PC2 keeps increasing and PC0 almost has no influence.

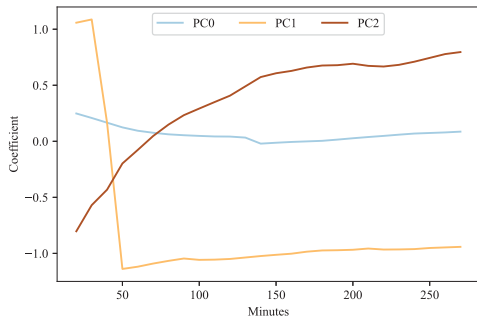


Fig. 10. Coefficients for PCA components

Negative likelihoods for three models are sketched in the figure 11. It suggests that more information enhances the likelihood of observing 200 failures and 3 components of PCA does not reduce any information from original covariates.

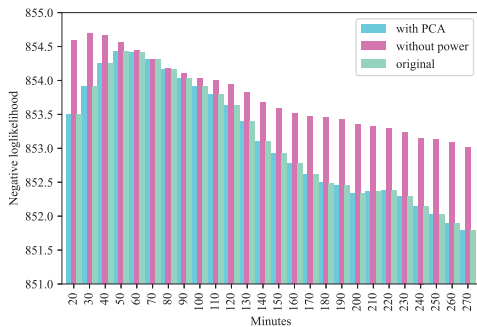


Fig. 11. Negative loglikelihood

5.4. Discussion of results

Based on results, wind positively increases hazard in the long run. However, power and temperature decrease it. Even if power is removed, temperature still has a negative coefficient. Model with PCs confirms factors that reduces the growth of hazard rate. There are some possible explanations:

In terms of failure cause, low temperatures lead to brittleness or freezing of lubricants, and tem-

perature variations cause material to expand or contract (Tavner et al., 2013). Because the turbine is located in the Gulf of Guinea, it is likely that tropical climate has a positive influence on turbine survival.

As for power, its coefficient changes from 0.5 to -0.5 and the reason behind could be grid adjustment. Negative loads represent wind generators can deliver current but voltage is imposed by electrical system at the connection point (Daniel et al., 2013). In the long run, this adjustment is good for improving the reliability of wind turbines.

All the three models suggest that accumulation duration influences the power of co-variates on hazard rate. The more information fed into the model, the more stable the power of the covariates. Short-term observations are not sufficient to produce robust results.

There are several limitations to this study. The first limitation is the lack of prediction and maintenance optimisation. The second limitation is that synergistic effects of variables and unobserved variables were not investigated. Future work can include adjusting the accumulation period, adding unobserved factors or other signal variables.

6. Conclusions and future work

This paper presents a comprehensive statistical analysis of the failure associated with a single offshore wind turbine. Seven statistical indices are utilized to evaluate the type of failure process. The Cox model is employed to model the process, and three forms of covariates are utilized. The main conclusions of the current work can be itemized as follows:

- The failure process of the investigated turbine has been shown to be a non-homogeneous Poisson process with a non-monotonic trend.
- In the long run, the growth of hazard rate is accelerated by the maximal wind, while the growth is delayed by the average temperature and the power condition.
- The influence of temperature, wind, and power on hazard rate growth varies with the accumulation duration.

In summary, the performance of Cox model is sat-

isfying and results can be used as reference Future work will focus on extension of Cox model such adding unobserved co-variates, failure prediction and maintenance optimization.

Acknowledgement

This publication has been prepared as part of North-Wind (Norwegian Research Centre on Wind Energy) co-financed by Research Council of Norway, industry and research partners.

References

- Adumene, S. and H. Ikue-John (2022). Offshore system safety and operational challenges in harsh Arctic operations. *Journal of Safety Science and Resilience* 3(2), 153–168.
- Antoch, J. and J. Daniela (2007). Testing a Homogeneity of Stochastic Process. *Kybernetika* 43, 415–430.
- Carroll, J., A. McDonald, and D. McMillan (2016). Failure rate, repair time and unscheduled O&M cost analysis of offshore wind turbines: Reliability and maintenance of offshore wind turbines. *Wind Energy* 19(6), 1107–1119.
- Cevasco, D., S. Koukoura, and A. Kolios (2021). Reliability, availability, maintainability data review for the identification of trends in offshore wind energy applications. *Renewable and Sustainable Energy Reviews* 136, 110414.
- Cockeran, M., S. G. Meintanis, and J. S. Allison (2021). Goodness-of-fit tests in the Cox proportional hazards model. *Communications in Statistics - Simulation and Computation* 50(12), 4132–4143.
- D'Agostino, R. B. and M. A. Stephens (1986). *Goodness-of-fit techniques*, Volume 68. Dekker.
- Daniel, R., P. Eugenio, and R. Julian (2013). Wind Farms as Negative Loads and as Conventional Synchronous Generation – Modelling and Control. In S. M. Mueen (Ed.), *Modeling and Control Aspects of Wind Power Systems*. InTech.
- Kaidis, C., B. Uzunoglu, and F. Amoiralis (2015). Wind turbine reliability estimation for different assemblies and failure severity categories. *IET Renewable Power Generation* 9(8), 892–899.
- Kiefer, J. (1959). K-sample analogues of the Kolmogorov-Smirnov and Cramér-V. Mises tests. *The Annals of Mathematical Statistics* 30, 420–447.
- Kvaløy, J. T. and B. H. Lindqvist (2003). A Class of Tests for Renewal Process Versus Monotonic and Nonmonotonic Trend in Repairable Systems Data. In *Series on Quality, Reliability and Engineering Statistics*, Volume 7, pp. 401–414. World Scientific.
- Li, H., W. Peng, C. Huang, and C. Guedes Soares (2022). Failure Rate Assessment for Onshore and Floating Offshore Wind Turbines. *Journal of Marine Science and Engineering* 10(12), 1965.
- Lin, D. Y. (2007). On the Breslow estimator. *Lifetime Data Analysis* 13(4), 471–480.
- Lindqvist, B. H., G. Elvebakk, and K. Heggland (2003). The Trend-Renewal Process for Statistical Analysis of Repairable Systems. *Technometrics* 45(1), 31–44.
- Menezes, D., M. Mendes, J. A. Almeida, and T. Farinha (2020). Wind Farm and Resource Datasets: A Comprehensive Survey and Overview. *Energies* 13(18), 4702.
- Reder, M., N. Y. Yürüşen, and J. J. Melero (2018). Data-driven learning framework for associating weather conditions and wind turbine failures. *Reliability Engineering & System Safety* 169, 554–569.
- Slimacek, V. and B. H. Lindqvist (2016a). Nonhomogeneous Poisson process with nonparametric frailty. *Reliability Engineering & System Safety* 149, 14–23.
- Slimacek, V. and B. H. Lindqvist (2016b). Reliability of wind turbines modeled by a Poisson process with covariates, unobserved heterogeneity and seasonality: Rate of occurrence of failures of wind turbines. *Wind Energy* 19(11), 1991–2002.
- Slimacek, V. and B. H. Lindqvist (2017). Nonhomogeneous Poisson process with nonparametric frailty and covariates. *Reliability Engineering & System Safety* 167, 75–83.
- Su, C., Q. Jin, and Y. Fu (2012). Correlation analysis for wind speed and failure rate of wind turbines using time series approach. *Journal of Renewable and Sustainable Energy* 4(3), 032301.
- Tavner, P., C. Edwards, A. Brinkman, and F. Spinato (2006). Influence of Wind Speed on Wind Turbine Reliability. *Wind Engineering* 30(1), 55–72.
- Tavner, P., D. Greenwood, M. Whittle, R. Gindele, S. Faulstich, and B. Hahn (2013). Study of weather and location effects on wind turbine failure rates: Study of weather and location effects. *Wind Energy* 16(2), 175–187.
- Tavner, P. J., J. Xiang, and F. Spinato (2007). Reliability analysis for wind turbines. *Wind Energy* 10(1), 1–18.
- Vaurio, J. K. (1999). Identification of process and distribution characteristics by testing monotonic and non-monotonic trends in failure intensities and hazard rates. *Reliability Engineering and System Safety* 64, 345–357.
- Wilkinson, M. and G. G. Hassan (2011). Measuring Wind Turbine Reliability - Results of the Reliawind Project. *Wind Energy* 35, 102–109.
- Wilson, G. and D. McMillan (2013, September). Modeling the relationship between wind turbine failure modes and the environment. In R. Steenbergen, P. van Gelder, S. Miraglia, and A. Vrouwenvelder (Eds.), *Safety, Reliability and Risk Analysis*, pp. 801–809. CRC Press.